Effect of disorder on the magnetic properties of $SmCo_5$

Diandra L. Leslie-Pelecky
Department of Physics and Astronomy and Center for Materials Research & Analysis, University of Nebraska, Lincoln, Nebraska 68588-0111

R. L. Schalek*
Department of Mechanical Engineering and Center for Materials Research & Analysis, University of Nebraska, Lincoln, Nebraska 68588-0656

(Received 15 April 1998; revised manuscript received 14 July 1998)

Mechanical milling of initially ordered ferromagnetic $SmCo_5$ produces dramatic increases in coercivity after short (15 min to 1 h) milling times, accompanied by remanence ratios on the order of 0.7 and shifted hysteresis loops. X-ray diffraction shows that milling induces both chemical and structural disorder. The hysteresis-loop shift is continuous and nonlinear with temperature over the range 5–300 K. The high coercivities are attributed to the formation of a nanostructure consisting of crystalline $SmCo_5$ regions separated by a disordered interphase. [S0163-1829(99)02001-9]

I. INTRODUCTION

Magnetic nanostructures often exhibit distinctly different behavior than their bulk counterparts.[1] Although there are many techniques for fabricating nanostructured magnetic materials, mechanical milling has emerged as a unique method of producing disorder in intermetallic alloys.[2–5] Mechanical milling is a high-energy deformation process that progressively introduces defect structures (dislocations and vacancies), atomic-scale chemical disorder and elastic strain energy into the initially crystalline starting powders through the shearing actions of ball-powder collisions.

$SmCo_5$ is a magnetic intermetallic alloy with a large anisotropy (1.3×10^8 ergs/cm^3). The $CaCu_5$ hexagonal crystal structure of $SmCo_5$ permits a close crystallographic relationship with the Sm_2Co_{17} crystal structure. The Sm_2Co_{17} structure, which is also magnetic, is derived from the $SmCo_5$ structure by the ordered substitution of each third Sm atom in the basal plane with a (dumbbell) pair of Co atoms. This simple crystallographic relationship, combined with a high potential for production of high-energy-product magnets and thin-film devices,[6] makes $SmCo_5$ an interesting material in which to study the effect of disorder on magnetism.

Section II describes sample fabrication and the experimental techniques used to investigate the nanostructure and magnetic properties of the milled material. Measurements of the coercivity, remanence ratio, and saturation magnetization as functions of milling time and temperature are found in Sec. III. Section IV presents a discussion of the possible mechanisms responsible for the observed high coercivities and shifted hysteresis loops. Conclusions are presented in Sec. V.

II. EXPERIMENTAL PROCEDURE

The commercially purchased $SmCo_5$ powder (-100 mesh) was handled exclusively in an argon-filled glove box to prevent oxidation. Milling was performed in a hermetically sealed tungsten-carbide-lined vial in a SPEX 8000 mixer/mill. Milling was stopped every 15 min for the first 2 h and every hour thereafter to remove a small amount of powder for x-ray-diffraction and magnetic measurements, and to break up clumps of powder.

Magnetic measurements were made using a superconducting quantum interference device magnetometer. Samples were loaded in paraffin-filled polyethylene bags in the glove box and sealed. The paraffin was melted to immobilize the randomly oriented powder particles during measurement. The coercivity, H_c, magnetization at 55 kOe, M_s, and remanence ratio, M_r/M_s, were extracted from the hysteresis loops. Not all hysteresis loops were fully saturated at 55 kOe, so the value of M_s is in some cases an approximate saturation magnetization.

X-ray-diffraction (XRD) patterns were obtained using a D-Max-B Rigaku diffractometer with Cu $K\alpha$ radiation. XRD is the only technique in which the particles are exposed to the air during measurement. The measured (110) diffraction peak was Fourier decomposed and compared to a LaB_6 standard to remove instrumental broadening and contributions from the $K\alpha_2$ doublet using the Stokes technique.[7] A single-profile analysis[8] that separates linewidth broadening due to microstrain from broadening due to grain size was applied to extract the coherent diffracting crystallite size (DCS) and root-mean-squared microstrain.

Bright-field transmission electron micrographs (TEM) were taken using a JEOL 2010 high-resolution microscope operating at 200 kV. TEM sample preparation consisted of encapsulating milled powder in a room-temperature-cured epoxy and microtoming with a diamond knife to a thickness of approximately 100 nm.

III. RESULTS

A. Structure

Figure 1 shows the x-ray-diffraction patterns of $SmCo_5$ as function of milling time. The unmilled powder exhibits sharp diffraction peaks corresponding to $SmCo_5$.[9] The fundamental hcp lines broaden as the milling time increases. After 10 h,

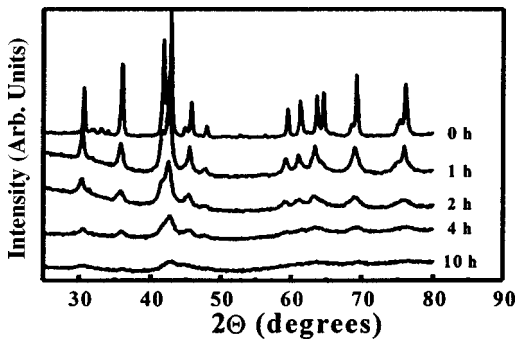

FIG. 1. X-ray-diffraction patterns for mechanically milled $SmCo_5$ powders for times of (top to bottom) 0, 1, 2, 3, 4, and 10 h.

only the (111) peak has appreciable intensity, indicating a nearly amorphous structure. Very broad peaks corresponding to fcc or highly faulted hcp cobalt are observed for milling times greater than 25 h. Differential broadening of the XRD peaks is observed and is likely due to strain energy stored in grain boundaries and other defect regions.[10,11]

Figure 2 shows the dependence of the DCS and the root-mean-squared (rms) microstrain on milling time. The solid curve through the DCS data represents an exponential decay that is characteristic of diffusion-induced disordering. The rms microstrain was calculated at an averaging distance of 3 nm. Calculations of the DCS and microstrain for longer milling times were not possible due to the extreme breadth and low intensity of the peaks. Note that the x-ray line-broadening analysis yields the size of coherent diffracting regions. These regions might be actual grains with high-angle grain boundaries, but could also be due to accumulated dislocation networks that interrupt lattice regularity. The large microstrain and relatively small DCS values of the starting powder result from the introduction of a large dislocation density when the as-cast $SmCo_5$ is ground to the appropriate particle size in the powder production process.

Figure 3 shows a TEM micrograph of $SmCo_5$ powder milled for 2 h. Several similar samples were imaged and show that the $SmCo_5$ particles produced by milling have an average diameter of about 30 nm. The 30-nm figure represents a lower bound, as the TEM micrograph is a two-dimensional representation of a three-dimensional object and a bias toward small particles is introduced when preparing the TEM samples through selection of particles that facilitate successful microtoming. Though qualitative, these observations suggest that the overall particle size is larger than the

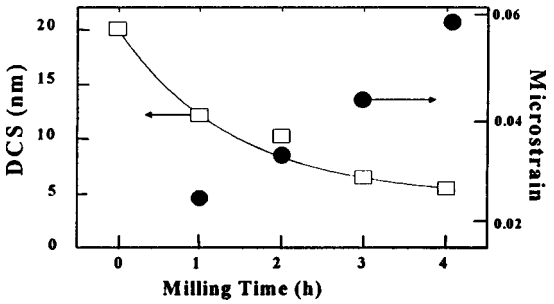

FIG. 2. The coherent diffracting crystallite size (DCS) and root-mean-squared microstrain obtained from the (110) x-ray-diffraction peak as a function of milling time.

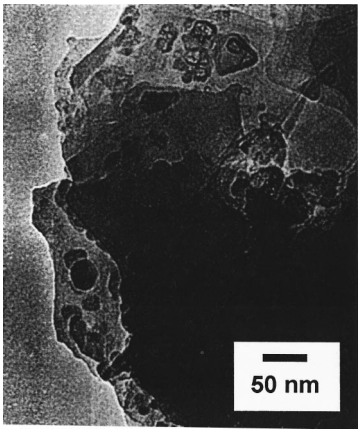

FIG. 3. Transmission electron micrograph of $SmCo_5$ milled for 2 h. The powders were encased in epoxy and microtomed prior to imaging.

DCS value obtained by x-ray diffraction (10 nm). Mechanical milling thus produces nanostructured particles with multiple coherent diffracting regions in the interior of the particles separated by a defect-laden or disordered region.

B. Magnetic properties

Figure 4 shows representative hysteresis loops at 300 K (left column) and 5 K (right column) for milling times of 0.25 h (top row), 2 h (middle row), and 10 h (bottom row).

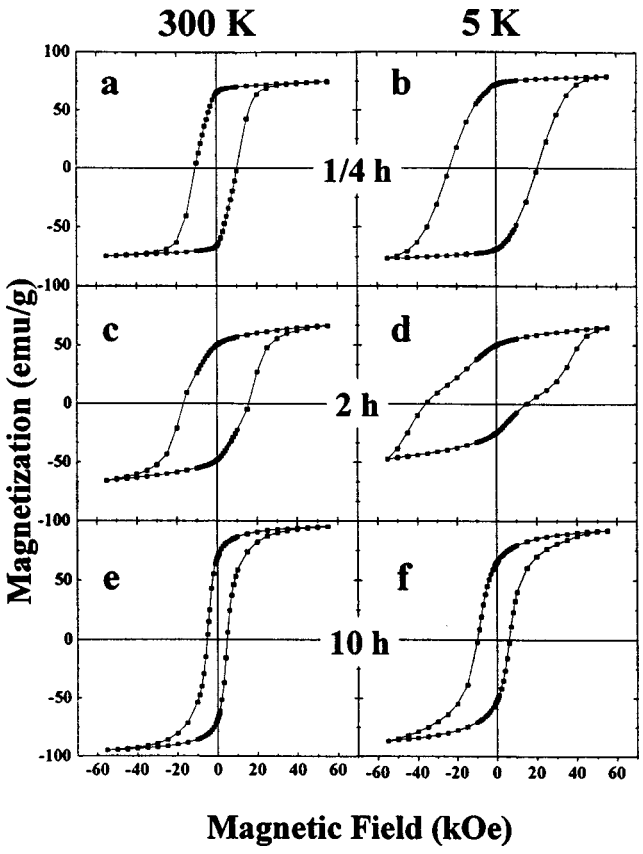

FIG. 4. Representative hysteresis loops from samples milled for 0.25 h (a) and (b), 2 h (c) and (d), and 10 h (e) and (f). (a), (c) and (e) are measurements taken at room temperature while (b), (d), and (f) were taken at 5 K.

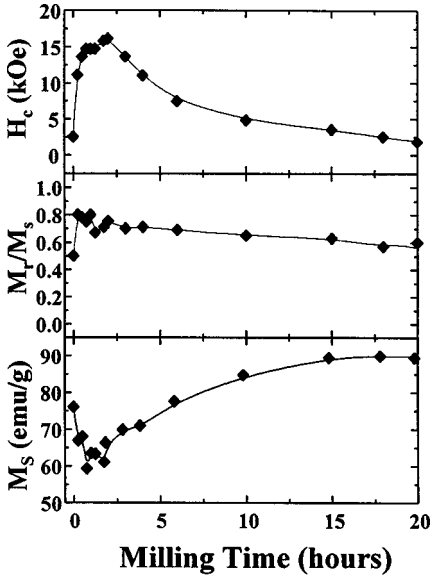

FIG. 5. The dependence of the room-temperature coercivity (H_c), remanence ratio (M_r/M_s), and saturation magnetization (M_s) on milling time.

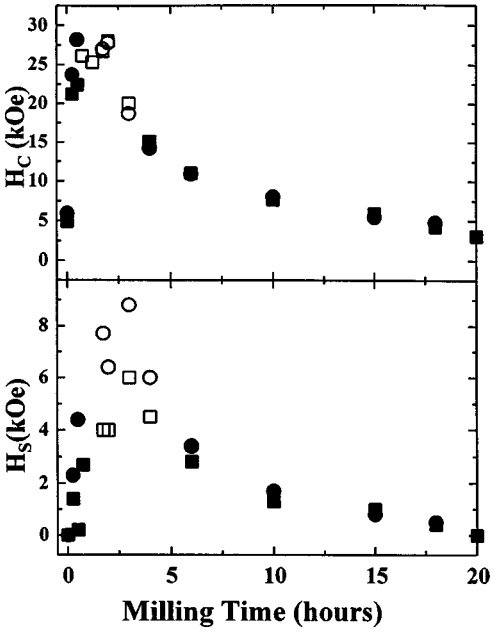

FIG. 6. The dependence of the coercivity (H_c) and hysteresis loop shift (H_S) on milling time for samples measured at 100 K (squares) and 5 K (circles). Open symbols represent measurements in which the hysteresis loop was not fully saturated.

Three features are noted. (1) the room-temperature coercivity H_c increases rapidly from the 2.5 kOe of the unmilled powder to 10 kOe after only 15 min of milling. The room-temperature remanence ratio M_r/M_s increases from 0.5 in the unmilled powder to 0.75 after 15 min of milling. (2) The sample milled for 2 h appears single phase at room temperature [Fig. 4(c)], but shows two-phase behavior at lower temperatures [Fig. 4(d)]. Low-temperature two-phase hysteresis loops are observed in samples milled from 1 to 4 h. Hysteresis loops from these samples are in general not saturated at the maximum field of 55 kOe. (3) Low-temperature hysteresis loops—taken after cooling in a field of 55 kOe—show a distinct shift toward negative field in all samples milled for times up to 20 h.

Figure 5 summarizes the dependence of the room-temperature H_c, M_r/M_s, and saturation magnetization, M_s, on milling time. H_c reaches a maximum value of 16 kOe after 2 h of milling then decreases monotonically with continued milling. M_r/M_s remains above 0.5 for milling times up to 22 h. M_s decreases for the first 2 h of milling then increases, returning to the value of the unmilled material after 6 h of milling. The increase in M_s for longer milling times may be a consequence of cobalt precipitation driven by the combined effects of diffusion and defect coalescence. Small amounts of cobalt are observed in the x-ray-diffraction patterns of samples milled for 28 h or longer. All analyses presented here are made on samples milled $\leqslant 20$ h to eliminate the possibility of elemental cobalt in the sample. A similar dependence of the coercivity on milling time is observed in mechanically milled $Sm_2(Co,Fe)_{17}$, although the interpretation is more complicated due to multiple phase changes in the material during the milling period investigated.[12]

Hysteresis loops measured below room temperature exhibit a shift H_s to negative fields. Figure 6 compares the coercivity (a) and loop shift (b) as functions of milling time. Squares represent data taken at 100 K and circles represent data taken at 5 K. Open symbols designate samples in which two-phase, nonsaturated behavior was observed. The quantity plotted as H_c is the half width of the hysteresis loop $H_{1/2}=\frac{1}{2}(H_L+H_R)$, where H_L and H_R are the left and right intercepts of the hysteresis loop with the field axis. The loop shift is defined as $H_S=H_L-H_{1/2}$. M_s and M_r/M_s did not differ significantly from the room-temperature data and are not shown. H_S ranges from 300 Oe for the unmilled sample to a maximum of 9 kOe in the 2-h milled sample at 5 K. The lack of saturation may lead to uncertainty in H_C and H_S in some samples.

Samples with large coercivities have an asymmetry in the values of the magnetization at $+55$ kOe and -55 kOe, suggesting that these measurements are only minor loops. The observed shift may then be a consequence of incomplete saturation; however, samples with lower coercivities and symmetry in the saturation magnetization values still show distinct shifts toward the negative field axis. The cited coercivity of incompletely saturated sample is thus a lower limit; however, the data for completely saturated samples support the correlation shown in Fig. 6.

Figure 7 compares H_S and H_c as functions of temperature for a 6-h milled sample. The 6-h milled sample was chosen for study as it does not exhibit two-phase behavior over the temperature range 5–300 K. Data were taken after cooling in a 55-kOe field. The remanence ratio varies little with temperature and is not shown. The solid line in Fig. 7(a) shows that the shift is nonlinear and continuous with temperature.

Figure 8 shows the field-cooled (FC) and zero-field-cooled (ZFC) magnetization as functions of temperature for the 6-h-milled sample. The measuring and cooling fields were 100 Oe. There is a broad peak near 175 K in both the FC and the ZFC data, and a broad peak in the ZFC data near 20 K without a corresponding peak in the FC data. Analysis of the field dependence of the peak is complicated by the

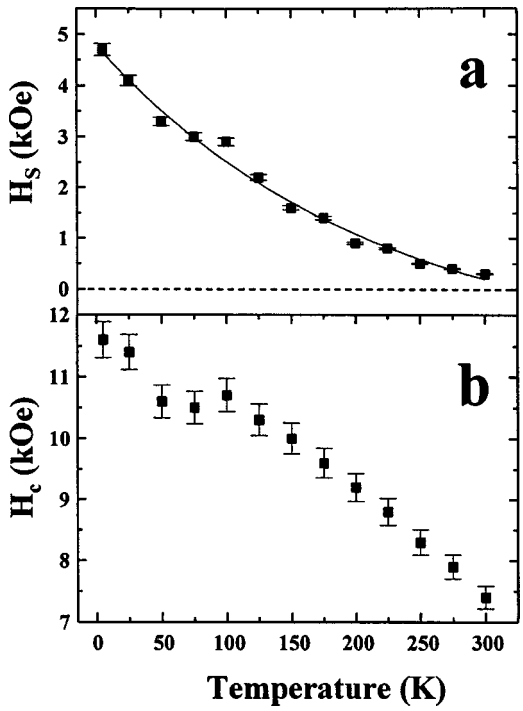

FIG. 7. Temperature dependence of the field shift (a) and coercivity (b) as functions of temperature for a sample milled for 6 h. The solid lines illustrate the continuous behavior of the shift and the coercivity with temperature.

ferromagnetic contribution, which dominates the weaker irreversible behavior when the external field is large.

IV. DISCUSSION

Mechanical milling introduces dislocations and vacancies, and increases the local microstrain. In ordered alloys, such as $SmCo_5$, mechanical milling also introduces atomic-level disordering of the alloy, especially in the early stages of milling.[2,3] The structural and magnetic characterization of the milled material suggests a nanostructure similar to that of Fig. 9, in which the gray regions represent crystalline $SmCo_5$ and the white regions represent a glassy, disordered Sm-Co mixture. Similar representations of mechanically milled materials have been proposed previously.[13,14] Arrows indicate the magnetocrystalline anisotropy of the $SmCo_5$. Increasing

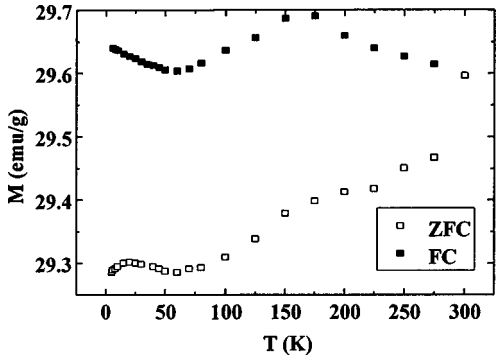

FIG. 8. Field-cooled (solid squares) and zero-field-cooled (open squares) magnetization as a function of temperature for a sample milled for 6 h. Data were measured in a field of 100 Oe.

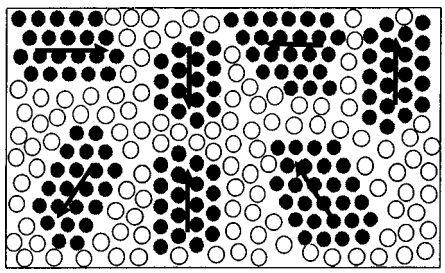

FIG. 9. Schematic illustration of the proposed nanostructure, with dark circles representing grains, arrows representing the anisotropy within the grain, and open circles representing a glassy interphase region.

the milling time converts a larger fraction of the sample to the disordered phase, consistent with the disappearance of crystalline peaks in the x-ray-diffraction patterns. At very long milling times, cobalt precipitates from the disordered phase. Extended x-ray-absorption fine structure shows that mechanically milled $Sm_2(Co,Fe)_{17}$ compounds exhibit segregation of Sm to the grain boundaries after prolonged milling.[12]

Glassy magnetic behavior has been observed in a number of mechanically milled ferromagnets, including $GdAl_2$ (Refs. 2 and 3) and Co_2Ge.[15] The $SmCo_5$ system is slightly more complicated to analyze because complete transformation to a glassy phase is not possible due to cobalt precipitation. The FC-ZFC magnetization measurements of Fig. 8 show a combination of ferromagnetic behavior and the characteristic irreversibility of glassy materials. (The measurements analyzed in this paper are all taken on samples with milling times much less than that at which cobalt precipitates are first observed.) Both high-anisotropy amorphous[16,17] and substituted $SmCo_5$ compounds (e.g., $SmCo_{5-x}Ni_x$, $SmCo_{5-x}Cu_x$)[18,19] have locally fluctuating magnetic interactions that lead to very high coercivities. A similar mechanism introduced via local disorder may be responsible for the behavior of $SmCo_5$; however, the characteristic dependence of the coercivity in substituted $SmCo_{5-x}M_x$ alloys ($H_c \propto T^{1/2}$) is not observed in mechanically milled $SmCo_5$.[20]

Skomski *et al.* have proposed[21] that unidirectional anisotropy produced by low symmetry can produce shifted hysteresis loops, even in the absence of antiferromagnetic coupling. Shifted hysteresis loops have been observed in very thin films of Co on Cu.[22] The atomic-level disorder of $SmCo_5$ could produce a macroscopic unidirectional anisotropy due to competing anisotropy coefficients, or to a Dzyaloshinskii-Moriya–type anisotropy. The unidirectional anisotropy could be operational at the atomic scale or on the scale of individual nanocrystals, in analogy with random anisotropy systems.[23]

Grain refinement can produce significant changes in the coercivity;[24] however, grain refinement alone cannot explain all of the observed data for mechanically milled $SmCo_5$. For example, two-phase hysteresis loops and loop shifts cannot be attributed to grain size effects. Further evidence against grain size refinement as the mechanism for coercivity enhancement is found in the time dependence of the magnetization as samples are aged after fabrication. We find significant changes in the half width of the hysteresis loop in the first two weeks following milling, but no corresponding

change in the x-ray-diffraction linewidth.[25] During the ageing time, the saturation magnetization decreases by only 0.7%, confirming that the effect is not due to oxidation. The loop half width becomes constant after about two weeks. (All of the data analyzed in this paper were acquired only after the loop half widths had reached constant values.) Ageing has little effect on the remanence ratio. The coercivity of a sample milled for 0.25 h changes from 15 to 9 kOe after 5000 min of ageing, with no change in the x-ray linewidth.

As-fabricated elemental nanostructures have a significant fraction of atoms that are not located on crystalline lattice sites. As the sample ages, room-temperature reorganization of the atomic structure occurs as disordered atoms move to crystalline lattice sites.[26] This change in structure is not reflected in the x-ray-diffraction linewidth, but can be identified through analysis of the x-ray atomic distribution function[26] or TEM.[27] Although most of the mechanical energy in the milling process is converted to heat, some energy is stored in the powder and released by recovery and recrystallization mechanisms. Recrystallization generally occurs at temperatures above 0.5 times the melting temperature;[28] however, room-temperature recrystallization has been observed in electrodeposited Cu films.[27] Recovery occurring at room temperature is accomplished by the removal of point defects such as vacancies, substitutional atoms, and antisite atoms. This is thus a reordering process and not a cause of grain growth.

Two additional mechanisms involving coupling between multiple phases must be examined. Exchange coupling between hard and soft magnetic phases produces large coercivities and remanence ratios above 0.5;[29] however, there are, to our knowledge, no reports in the literature showing shifted hysteresis loops. No identifiable second phase is observed via x-ray diffraction in the samples with large coercivities and the characteristic ''exchange-spring'' reversibility of the hysteresis loop for $H<H_c$ is absent.

Ferromagnetic-antiferromagnetic (F-AF) coupling can produce high coercivities and shifted hysteresis loops.[30] Compositional inhomogeneities giving rise to competing interactions can produce shifted hysteresis loops in bulk materials; however, there must be a source of antiferromagnetic interactions.[31] The oxidation of $SmCo_5$ is selective for samarium;[32] however, no order has been found in samarium oxides between room temperature and 6 K.[33] The Néel temperature of CoO is 291 K; however, nanoscale Co:CoO particles show a finite-size depression of the Néel temperature to 150 K.[30] Samples purposely contaminated by the introduction of a small amount of air during milling have Sm and Co oxides detectable by XRD, significantly lower coercivities than the protected samples, and no loop shifts at room temperature. No evidence of oxide formation is observed in XRD patterns. Within the sensitivity of energy-dispersive x-ray analysis ($\sim$1 at. %), no contamination from the milling media (tungsten or carbon) or from oxygen is evident.

Shifted hysteresis loops in F-AF exchange-coupled systems occur only when the system is cooled in a magnetic field below the Néel temperature of the antiferromagnet. No shift in the hysteresis loop is observed above the Néel temperature, or when the sample is cooled without a field.[34] In contrast, Fig. 7(a) shows that the $SmCo_5$ hysteresis-loop shifts are continuous with temperature in the range 5–300 K. Milled $SmCo_5$ is very sensitive to sample measurement history: samples must be carefully field demagnetized to show that there is no shift when cooled in zero field. To determine whether there was a cutoff temperature below which the application of a field did not produce a shift, we cooled a sample without a field to a target temperature T_x then applied a 55-kOe field and continued cooling to 5 K. A shift in the hysteresis loop is observed for all $T_x \geqslant 50$ K, although the magnitude of the shift decreases as T_x decreases. This is in contrast to the behavior observed in Co:CoO systems.[35] Cooling from temperatures above 300 K is not possible due to recovery and grain growth of the sample and the softening of the paraffin used as a fixative. We thus conclude that oxidation is not a primary cause of the observed magnetic behavior. Further measurements are necessary to determine whether the shifted hysteresis loops can be the result of hard-soft magnetic exchange coupling, or due to milling-induced disorder.

V. CONCLUSION

Structural and magnetic measurements of mechanically milled $SmCo_5$ suggest that milling produces small $SmCo_5$ crystallites separated by a glassy Sm-Co interphase. The volume fraction of the interphase increases with additional milling. The high coercivities and remanence ratios above 0.5 are similar to those in amorphous and site-disordered magnets with large anisotropy. Local interaction fluctuations increase the resistance to magnetization reversal; however, the temperature dependence of the coercivity is not the $T^{1/2}$ of substitutional $SmCo_{5-x}M_x$ compounds.

Ageing experiments show that the data are not consistent with grain size refinement. Although we cannot exclude oxidation—which could produce F-AF exchange coupling—with complete certainty, sample characterization and ageing studies suggest that oxidation is likely not the primary effect responsible for the changing magnetic properties. None of the typical behavior of hard-soft ferromagnetic exchange-coupled systems is observed; however, there has been little investigation of low-temperature hysteresis-loop shifts in these systems, so this mechanism cannot be entirely eliminated as a possibility. Further investigation of disordered magnetic alloys, including detailed understanding of the dependence of the coercivity on temperature, is important to fundamental understanding of coercivity mechanisms and for applications such as high-energy-product permanent magnetic materials.

ACKNOWLEDGMENTS

This work was supported by NSF Grant No. OSR 925525 and AFOSR Grant No. F49620-98-1-0098. We thank E. M. Kirkpatrick and R. Skomski for helpful comments and discussions. We especially thank D. J. Sellmyer for helpful discussions, suggestions, and critical reading of this paper.

*Present address: Composite Materials and Structures Center, Michigan State University, East Lansing MI 48824.
[1] D. L. Leslie-Pelecky and R. D. Rieke, Chem. Mater. **8**, 1770 (1996).
[2] G. F. Zhou and H. Bakker, Phys. Rev. B **52**, 9437 (1995).
[3] G. F. Zhou and H. Bakker, Phys. Rev. Lett. **73**, 344 (1994).
[4] R. H. Kodama, C. L. Seaman, A. E. Berkowitz, and M. B. Maple, J. Appl. Phys. **75**, 5639 (1994).
[5] R. H. Kodama, A. E. Berkowitz, E. J. McNiff, Jr., and S. Foner, Phys. Rev. Lett. **77**, 394 (1996).
[6] K. Kumar, J. Appl. Phys. **63**, R13 (1988).
[7] A. R. Stokes, Proc. Phys. Soc. London **61**, 382 (1948).
[8] P. Ganesan, H. K. Kuo, A. Saavedra, and R. J. DeAngelis, J. Catal. **52**, 310 (1978).
[9] Y. Kahn and D. Feldman, J. Less-Common Met. **31**, 211 (1973).
[10] D. L. Leslie-Pelecky, M. Bonder, T. Martin, E. M. Kirkpatrick, X. Q. Zhang, S.-H. Kim, and R. D. Rieke, IEEE Trans. Magn. **34**, 1018 (1998).
[11] E. Hellstern, H. J. Fecht, Z. Fu, and W. L. Johnson, J. Appl. Phys. **65**, 305 (1989).
[12] V. G. Harris, M. Liou, B. N. Das, V. M. Browning, J. E. Snyder, M. Rubinstein, S. H. Lawrence, R. Littleton, and D. P. Pappas, J. Appl. Phys. **81**, 5121 (1997).
[13] E. A. Stern, R. W. Siegel, M. Newville, P. G. Sanders, and D. Haskel, Phys. Rev. B **75**, 3874 (1995).
[14] H. J. Fecht, Phys. Rev. Lett. **65**, 610 (1990).
[15] G. F. Zhou and H. Bakker, Phys. Rev. Lett. **72**, 2290 (1994).
[16] G. C. Hadjipanayis and D. J. Sellmyer, Phys. Rev. B **23**, 3355 (1981).
[17] G. C. Hadjipanayis, D. J. Sellmyer, and B. Brandt, Phys. Rev. B **23**, 3349 (1981).
[18] H. Oersterreicher, F. T. Parker, and M. Misroch, J. Appl. Phys. **50**, 4273 (1979).
[19] H. Oersterreicher, F. T. Parker, and M. Misroch, Phys. Rev. B **18**, 480 (1978).
[20] T. Egami, Phys. Status Solidi A **19**, 747 (1973).
[21] R. Skomski, H. P. Oepen, and J. Kirschner, Phys. Rev. B **58**, 3223 (1998).
[22] W. Wagner, H. V. Swygenhoven, H. J. Höfler, and A. Wiedenmann, Nanostruct. Mater. **6**, 929 (1995).
[23] R. Alben, J. J. Becker, and M. C. Chi, J. Appl. Phys. **49**, 1653 (1978).
[24] B. D. Cullity, *Introduction to Magnetic Materials* (Addison-Wesley, Reading, MA, 1972).
[25] D. L. Leslie-Pelecky, E. M. Kirkpatrick, and R. L. Schalek, Nanostruct. Mater. (to be published).
[26] J. Löffler and J. Weissmüller, Phys. Rev. B **52**, 7076 (1995).
[27] J. Dille, J.-L. Delplancke, J. Charlier, and R. Winand, in *Grain Size and Mechanical Properties—Fundamentals and Applications*, edited by N. J. Grant, R. W. Armstrong, M. A. Otooni, T. N. Baker, and K. I. Shisaki, MRS Symposia Proceedings No. 362, (Materials Research Society, Pittsburgh, 1995), p. 231.
[28] R. E. Reed-Hill, *Physical Metallurgy Principles* (van Nostrand, New York, 1973).
[29] E. F. Kneller and R. Hawig, IEEE Trans. Magn. **27**, 3588 (1991).
[30] W. H. Meiklejohn, J. Appl. Phys. **33**, 1328S (1962).
[31] J. S. Kouvel, J. Appl. Phys. **31**, 142S (1960).
[32] R. W. Bartlett and P. J. Jorgensen, Metall. Trans. A **5**, 355 (1974).
[33] S. J. Collocott and A. M. Stewart, J. Phys.: Condens. Matter **4**, 6743 (1992).
[34] S. Gangopadhyay, G. C. Hadjipanayis, C. M. Sorensen, and K. J. Klabunde, J. Appl. Phys. **73**, 6964 (1993).
[35] S. Gangopadhyay, G. C. Hadjipanayis, C. M. Sorensen, and K. J. Klabunde, IEEE Trans. Magn. **29**, 2602 (1993).